Inclusion of a Supercapacitor Energy Storage System in DFIG and full-converter PMSG Wind Turbines for Inertia Emulation

Alberto Berrueta, *Member, IEEE,* Javier Sacristán, Jesús López, *Member, IEEE,* José Luis Rodríguez, Alfredo Ursúa, *Senior Member, IEEE*, and Pablo Sanchis, *Senior Member, IEEE*

***Abstract*— The energy transition towards renewables must be accelerated to achieve climate targets. To do so, renewable power plants, such as wind power plants (WPPs) must replace conventional power plants (CPPs). Transmission System Operators require this replacement to be made without weakening the frequency response of power systems, so it must be ensured that WPPs match the response of CPPs to grid frequency variations. CPPs consist of grid-tied synchronous generators that inherently react to frequency variations by modifying their stored kinetic energy and their output power, thereby contributing to grid stability. Such response is known as inertial response. By contrast, wind turbines (WTs) are mostly based on either doubly-fed induction generators (DFIG) or permanent magnet synchronous generators (PMSG). Their power electronics interface decouples the electromechanical behavior of the generator from the power grid, leading to a negligible inertial response. Therefore, in order to replace CPPs with WPPs, WTs must be able to react to frequency variations by changing their output power, i.e., emulating an inertial response. Currently implemented inertia emulation strategies in WTs rely on pitch control and stored kinetic energy variation. This paper proposes an alternative strategy, using the energy stored in a supercapacitor directly connected to the back-to-back converter DC link to emulate inertia. Its performance is validated by means of simulation for both DFIG and PMSG. Compared to state-of-the-art techniques, it allows a more accurate emulation of grid-tied synchronous generators, favoring the replacement of these generators by WTs.**

Index Terms*— *Frequency, Energy storage, Inertia emulation, Synthetic inertia, Supercapacitor, Wind power generation.

I. Introduction

In an electrical power system, an imbalance between generated and consumed power causes a frequency variation. To ensure the stability and safe operation of the power system, the Transmission System Operator (TSO) controls the frequency to remain within a strict range. To do so, conventional generation plants automatically adjust their generated power to compensate for any imbalance, thereby avoiding large frequency excursions. This grid service is known as primary regulation. Any power controller used to provide primary regulation has inherent delays, so a change in system frequency is unavoidable in the first moments after the imbalance.

A grid-tied synchronous generator rotates at a speed defined by the grid frequency, i.e., it is coupled to the grid. Therefore, a frequency variation causes a change in its rotational speed, thereby modifying the kinetic energy stored in the rotating mass. For instance, in the event of a frequency drop caused by increased demand, the synchronous generator decelerates, releasing a fraction of its stored kinetic energy and injecting it into the grid. This inherent response contributes to the grid stability, compensating the initial increase in demand and attenuating the Rate of Change of Frequency (RoCoF). The variation of its stored kinetic energy caused by a change in frequency is known as inertial response (IR) [1].

Wind turbines (WTs) are not based on grid-tied synchronous generators. Most are based on doubly-fed induction generators (DFIG) or permanent magnet synchronous generators (PMSG). These generation topologies include power converters. Regarding PMSGs, the power converter completely decouples the electric generator and its electromechanical behavior from the power grid. This implies that they do not experience a natural variation in their stored kinetic energy due to a frequency change, i.e., they do not contribute with an IR. By contrast, a DFIG is sensitive to frequency events, but the implemented control loops, which are responsible for operating the WT at the maximum power point (MPP), make the IR insignificant [2], [3].

Wind power plants (WPPs) are continuously replacing conventional power plants based on synchronous generators [4], thereby reducing the system inertia. Thus, in order to maintain the increasing wind power penetration without weakening the frequency response, WTs need to be able to react to frequency variations by changing their output power. This ability is known as artificial, emulated, simulated or synthetic inertia [5].

A number of TSOs demand WPPs to emulate inertia as a requirement for grid connection. Hydro-Québec TransÉnergie (HQT) requires WPPs with a rated output power greater than 10 MW to be able to increase their active output power by at least 5% for about 10 s in response to severe frequency dips [6]. The Independent Electricity System Operator (IESO) in the Canadian province of Ontario has the same requirement for WPPs greater than 50 MW [6]. European Network of Transmission System Operators for Electricity (ENTSO-E) regulates that the TSOs shall have the right to require Type C power park modules (parks with connection point below 110 kV and maximum capacity at or above a threshold specified by each relevant TSO) to provide synthetic inertia during very fast frequency deviations [7]. Everything indicates that, over time, most TSOs will demand this type of performance from WPPs, so the study of how to

This work has been supported by Siemens Gamesa Renewable Energy, by the Spanish State Research Agency (AEI/10.13039/501100011033) under grants PID2019-111262RB-I00 and PID2019-110956RB-I00, and by the Government of Navarre under grant 0011-1411-2022-000049 (EnVeNA project). Any opinions, findings, and conclusions or recommendations expressed in this material are those of the authors and do not necessarily reflect those of Siemens Gamesa Renewable Energy.

Alberto Berrueta, Javier Sacristán, Jesús López, Alfredo Ursúa, and Pablo Sanchis are with the Institute of Smart Cities, Dept. of Electrical, Electronic and Communications Engineering, Public University of Navarre (UPNA), Campus de Arrosadía 31006 Pamplona, Spain (e-mail: alberto.berrueta@unavarra.es;javier.sacristan@unavarra.es; jesus.lopez@unavarra.es; alfredo.ursua@unavarra.es; pablo.sanchis@unavarra.es).

José Luis Rodríguez is with the Dept. of Onshore Electrical Module, Siemens Gamesa Renewable Energy, 31621 Sarriguren, Spain (e-mail: jose.l.rodriguez@siemensgamesa.com).

emulate an IR in WTs is, and will be, a key line of work for WT manufacturers.

Currently, the most common technique for inertia emulation (IE) in WTs (in both PMSG and DFIG) consists of varying the output power by modifying the pitch angle setpoint or allowing WT stored kinetic energy variations [8]. The main drawback of this IE technique is the modification of the turbine speed. The WT is forced away from the MPP, thereby reducing the captured the maximum available power [9]. Due to this reduction in the captured power during the recovery process, a secondary frequency drop (SFD) is likely to occur in a power grid with high wind penetration. In fact, the energy recovery of wind power plants performing this kind of inertial response may result in a severe SFD, with a frequency even lower than the initial event.

An alternative for this modified MPPT IE strategy is to include an energy-storage system (ESS) either inside each wind turbine or at plant level. Due to the undergoing technology evolution of Li-ion batteries [10], the most typical alternative for such ESS is a Li-ion battery, connected to the power converter DC link by means of a DC/DC converter, to the AC side of the converter by means of an inverter, or to the point of common coupling of the wind power plant by means of an inverter [11]. The main drawback of using a Li-ion battery is its limited durability, especially when it is operated under extreme ambient temperatures [12], [13]. Moreover, the power-to-energy ratio of commercial Li-ion batteries ranges from 0.2 to 5 h^{-1} [10], which is smaller than the requirements for inertia emulation of around 30 seconds (power-to-energy ratio of 120 h^{-1}) [1].

This paper proposes an IE technique for both PMSG and DFIG that keeps the turbine at the MPP, with no variation of its rotational speed, not requiring the use of a Li-ion battery, nor its associated power converter. The proposed system includes a supercapacitor (SC) directly connected to the DC link of the back-to-back power converter. SCs are energy storage systems with high power-to-energy ratio, extensive cycle life and decreasing costs that are being used in an increasing number of applications [14]. The power converter consists of two voltage-source converters (VSCs) connected through a bank of capacitors. The energy stored in the proposed SC is used to emulate the IR. The DC link voltage setpoint is the control variable to achieve this IR. Furthermore, this technique gets rid of limitations shown by conventional techniques, based on pitch control and stored kinetic energy variation.

The remaining of this paper is structured as follows. Section II describes the IR of a grid-tied synchronous generator. Section III is dedicated to discussing the IR of PMSG and DFIG WTs. Section IV analyses current techniques for emulating inertia in PMSG and DFIG WTs. The proposed IE strategy is presented in Section V, where its advantages over the conventional technique are also discussed. Section VI compares the performance of conventional and the proposed IE strategies in DFIG and PMSG WTs. Finally, Section VII summarizes the conclusions of the work.

II. Inertial Response of a Grid-Tied Synchronous Generator

The IR of a grid-tied synchronous generator can be divided into two stages [1].

A. Stage I: Rotor swings in the generators

In the very first instant after the disconnection of a generating unit, the remaining synchronous generators coupled to the grid provide a fast power peak. The power provided by each generator depends on its electrical distance from the disturbance. The larger the electrical distance from the disturbance, the lower the power provided. As the mechanical power provided by the prime mover remains constant, the additional power delivered to the grid is taken from its kinetic energy, thereby decelerating the machine. Due to the electromechanical behavior of the generator, this initial deceleration is followed by a sequence of continuous accelerations-decelerations, which result in swings in the generator's rotational speed, kinetic energy, and output power. Swings are attenuated due to the damping torque of the generator itself and are completely damped after a few seconds. Following this transient behavior, the output power is equal to the mechanical power provided by the prime mover, i.e., the generation loss is not compensated.

B. Stage II: Frequency drop

Once the described swings are damped, synchronous generators provide additional power that compensates the generation loss. This power is again taken from their kinetic energy. In this case, the magnitude of this contribution does not depend on the electrical distance from the disturbance. Each generator contributes with a power proportional to its kinetic energy. The inertia constant (H) of a generator is defined as its kinetic energy at synchronous speed divided by the machine power rating, as shown in (1):

$$H = \frac{\frac{1}{2} J \omega_{sm}{}^2}{S_n} \tag{1}$$

where J is the total moment of inertia of the turbine and generator rotor, ω_{sm} is the synchronous mechanical speed and S_n is the machine rated power. H is commonly expressed in seconds. Then, the generator's additional contribution during Stage II is proportional to its inertia constant and to its rated power.

Since the contribution of each generator is proportional to its stored kinetic energy, all generators slow down at approximately the same rate and, as the system frequency is directly linked to the speed of these generators, the frequency drops. Both the speed of the generators and the system frequency decrease until the primary regulation service compensates the generation-demand imbalance.

III. Inertial Response of DFIG and PMSG Wind Turbines

This section discusses the IR of a PMSG and a DFIG in their standard configurations, i.e., with no control loop for inertial emulation.

Any electric machine has an IR if a frequency change causes a variation in the machine's rotational speed (Ω). The machine varies its speed if the electromagnetic torque (T_{em}) is sensitive to changes in frequency[2].

Regarding a PMSG, the generator stator is connected to the grid via a back-to-back converter (AC/DC-DC/AC). The intermediate DC link included in the converter decouples the grid frequency from the frequency at the generator stator windings. Therefore, T_{em} is not sensitive to frequency variations, which leads to the conclusion that a PMSG in its standard configuration does not contribute with an IR.

By contrast, the stator of a DFIG is directly connected to the grid. To draw conclusions about its IR, the relationship between T_{em} and the grid frequency in this WT topology needs to be analyzed. The expression of DFIG T_{em} in a synchronous rotating reference frame oriented to the stator magnetic field is shown in (2):

$$T_{em} = -\frac{3}{2} p \frac{L_m}{L_s} \psi_s i_{qr} \quad (2)$$

where p is the number of pole pairs, L_m is its magnetizing inductance, L_s is the stator inductance (defined as the addition of stator leakage inductance and magnetizing inductance), ψ_s is the stator flux and i_{qr} is the rotor quadrature current (referred to the stator) [15].

At the same time, disregarding the small voltage drop in the stator resistance, ψ_s can be expressed as shown in (3):

$$\psi_s \approx \frac{v_s}{\omega_s} \approx \frac{v_s}{2\pi f} \quad (3)$$

where v_s is the stator voltage, ω_s is the synchronous electrical speed and f is the grid frequency [15]. These expressions show that T_{em} is sensitive to grid frequency changes. An analysis of (2) and (3) shows that ψ_s initially rises when the machine faces a frequency drop, causing an increase in T_{em}. Due to the torque imbalance, the DFIG decelerates, releasing a fraction of its stored kinetic energy and injecting it into the grid, leading to an increase in output power (P_{out}).

A WT (DFIG or PMSG) incorporates a control structure to ensure operation at the MPP, known as maximum power point tracking (MPPT). There are different strategies for implementing this control. Fig. 1 shows the general control schemes for three of the most widely implemented strategies [16]. When the DFIG incorporates the MPPT strategy shown in Fig. 1(a), the initial decrease in Ω causes a reduction in the output power reference (P^*_{out}). Even though both P^*_{out} and Ω are reduced, the electromagnetic torque setpoint (T^*_{em}) is reduced, given that P^*_{out} is proportional to the cube of Ω. In a DFIG, the rotor-side converter (RSC) incorporates a control

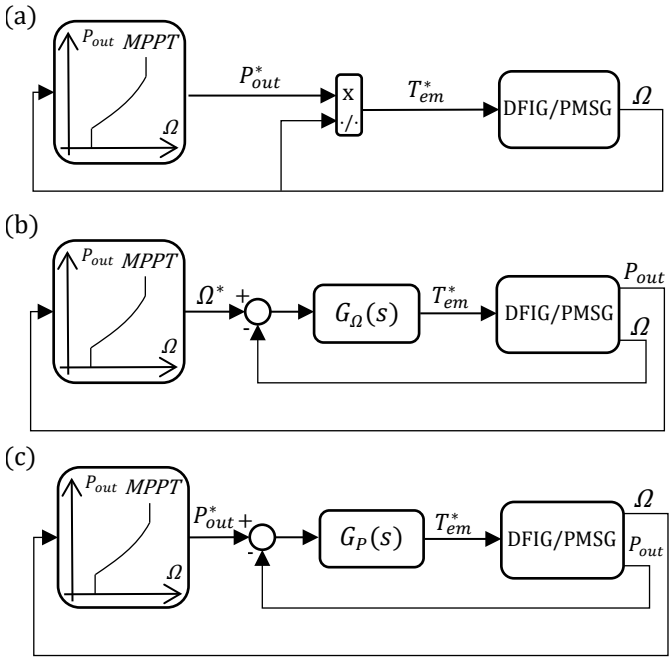

Fig. 1. Generalized control block diagrams of three state-of-the-art MPPT strategies for WTs: (a) open-loop control; (b) rotational speed closed-loop control; (c) output power closed-loop control.

that ensures that T_{em} follows T^*_{em}, thereby cancelling the IR. Then, the IR of a regular DFIG is insignificant.

If the DFIG includes the MPPT strategy shown in Fig. 1(b), the initial increase in P_{out} causes rotational speed setpoint (Ω^*) either to increase or to remain constant, depending on the WT operating point. If the WT operates in the variable-speed region, Ω^* increases, while it remains constant if the WT operates in the constant-speed region. In both cases, the initial deceleration sets Ω lower than Ω^*. The controller $G_\Omega(s)$ reacts to the speed error by decreasing the electromagnetic torque setpoint (T^*_{em}), trying to reduce the generator's braking torque that would lead to a rise in Ω. Again, the RSC ensures that T_{em} follows T^*_{em}, thereby cancelling the IR.

Analogously, if the implemented MPPT strategy is based on the scheme shown in Fig. 1(c), the initial decrease in Ω causes a reduction in P^*_{out}. Then, due to the first increase in P_{out}, it becomes higher than P^*_{out}. The controller $G_P(s)$ reacts to this power error by decreasing the value of T^*_{em}, in search of a machine acceleration. By doing so, the desired P_{out} reduction would be achieved, since a fraction of the mechanical power provided by the WT rotor would be devoted to the machine acceleration rather than being transformed into electrical power. As in the previous case, the RSC ensures that T_{em} follows T^*_{em}, cancelling the IR.

Therefore, with any state-of-the-art MPPT strategy, the magnitude and duration of the IR is determined by the speed of $G_\Omega(s)$ and $G_P(s)$ when reacting to speed and power errors, respectively, by modifying T^*_{em}. These controllers are tuned to only allow slight deviations of Ω around Ω^*. This controller tuning leads to variations in captured mechanical power being transformed into variations in stored kinetic energy. Given that rotating masses are mechanical power buffers, electrical power fluctuations are smoothed out [3], [17]. Given that only small deviations in Ω are allowed, the IR is insignificant.

IV. Inertia Emulation in DFIG and PMSG Wind Turbines

As explained above, WTs do not provide natural IR to the power grid. Therefore, a control system needs to be programmed to react to a frequency change by varying the WT's power, thereby emulating an IR.

The most common technique for IE in WTs consists of the following: the grid frequency is measured and filtered by means of a low-pass filter to reject measurement noise; the IE controllers receive the RoCoF or the frequency deviation from nominal value as input; depending on this input, they modify the electromagnetic torque, active power or rotation speed setpoint of the power converters and pitch angle control loops. This allows an active output power variation when frequency changes, thereby emulating an IR. In the event of a decrease in frequency, if WT is operating with rated output power, where the pitch angle is other than optimal, the IR is achieved by decreasing the pitch angle. However, if WT is operating with a power lower than the nominal value, with optimal pitch angle, the IR is achieved by extracting a fraction of its stored kinetic energy. This leads to a machine deceleration, causing an excursion from the MPP. This period of increased output power needs to be followed by a period of decreased power for the turbine to recover its original speed and MPP operation. This period is known as the recovery process [8], [18].

The state-of-the-art IE controllers [8] can be classified into three main categories: Natural Inertial Control (NIC), Step-wise Inertial Control (SIC) and Virtual Inertial Control (VIC)

[8]. In NIC, WT power is changed in proportion to RoCoF, frequency deviation or both. In SIC, upon detecting an under-frequency event, an over-power is delivered to the grid for several seconds. In VIC, when a frequency deviation is detected, the output power is rapidly regulated by switching the turbine operating point from the MPPT curve (with optimal power curve coefficient k_{opt}) to a VIC power tracking curve (with a variable curve coefficient k_{VIC} that is a function of the frequency deviation).

If NIC or SIC strategies are implemented, when the WT exits frequency regulation and starts the recovery process, the additional power drops directly to zero, and the output active power decreases instantaneously. This power shortage leads to an undesired Secondary Frequency Drop (SFD) after the Nadir frequency [19]. With VIC, during the recovery process, the VIC curve coefficient is continuously changed until it reaches k_{opt}, due to the continuous variation of the frequency deviation. Then, the recovery is a smooth process without sharp output power drops, thereby avoiding the SFD [8].

Fig. 2(a) shows the generalised control scheme for an open-loop MPPT that includes an NIC based on both RoCoF and frequency deviation from nominal value. Facing a decrease in frequency, the IE controller reacts by adding a contribution to the output power setpoint (ΔP^*_{out}). The same NIC-based IE controller included in a rotational speed closed-loop MPPT is shown in Fig. 2(b). In this case, the IE controller reacts to a frequency drop by modifying the T_{em} setpoint (ΔT^*_{em}) in order to control the deceleration of the machine and the release of stored kinetic energy to achieve the desired output power increase (ΔP^*_{out}). It is important to highlight the decrease in the reaction speed of the controller $G_\Omega(s)$ or $G_P(s)$ required to allow the machine deceleration during the frequency event [17]. The IE controller includes two dead bands, in order to ignore the continuous small perturbations in frequency that occur during the normal operation of the power system. Furthermore, it incorporates a high-pass filter to reject steady-state frequency errors.

There are different criteria for determining the value of constants $k_{df/dt}$ and $k_{\Delta f}$. Setting $k_{df/dt}=2\cdot H$ and $k_{\Delta f}=0$, ΔP^*_{out} can be expressed in p.u. as shown in (4):

$$\Delta P^*_{out} = -2Hf\frac{df}{dt} \tag{4}$$

where f is the grid frequency, in p.u.. This ΔP^*_{out} value matches with the additional output power that a grid-tied synchronous generator would supply during Stage II of its IR (described in Section II.B), as long as the generator has the same value of H. Therefore, with this selection of constants $k_{df/dt}$ and $k_{\Delta f}$, the WT mimics the IR of a grid-tied synchronous generator during Stage II of its dynamics [20].

The optimal value of $k_{df/dt}$ and $k_{\Delta f}$ for achieving the highest RoCoF attenuation and maximum Nadir frequency depends on the power system to which the WTs are connected. Different power system compositions have been analyzed in the literature, and the optimal $k_{df/dt}$ value has been found to be always close to zero [21]. Therefore, if $k_{df/dt}$ is set to zero, the optimal IR is calculated with no need for df/dt, which is a noise amplifying process and could result in undesired oscillations in P_{out}. In this scenario, the IE strategy is reduced to a fast droop control strategy, also known as Fast Frequency Response (FFR). It is also stated that the system's frequency response can be improved if conventional generators are replaced by WTs with this parameter fitting. Another study concludes that the most suitable pattern from a technical and robustness point of view is a Soft-Fast Frequency Response

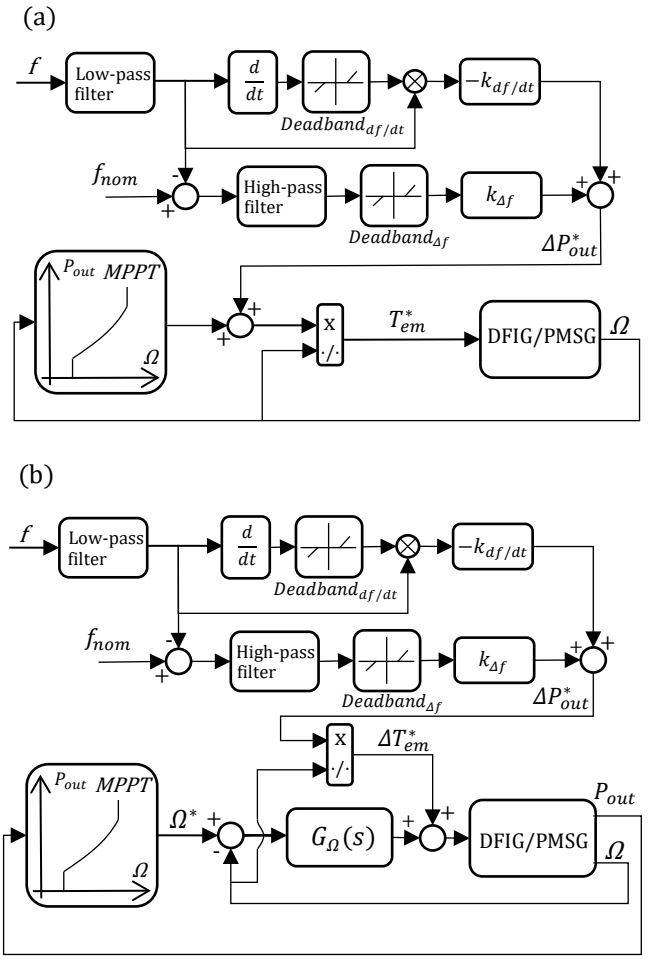

Fig. 2. Generalised control scheme of a NIC based on both RoCoF and frequency deviation included in: (a) an open-loop MPPT; (b) a rotational speed closed-loop MPPT.

(SFFR) [22]. This might be the reason that has led a number of WT manufacturers to choose the FFR technique for commercial inertia emulation controllers [6], [17].

Some authors have also suggested strategies that propose other energy sources to emulate inertia. An IE strategy for PMSG that simultaneously extracts kinetic energy from the rotating masses and stored energy from the DC link capacitor is proposed in [23]. However, as no additional Energy Storage System (ESS) is connected to the DC link, its contribution is limited. Alternatively, other authors propose two strategies for DFIG that rely on both WT rotational kinetic energy and energy from an SC coupled to the DC link [24]. In the former, both power sources are used simultaneously, while in the latter, the SC energy is used in the first place and the rotational kinetic energy is used later, via a cascading control, with this contribution having greater importance in the inertial response. Techniques for emulating inertia in a DFIG by connecting an SC in the DC link via an additional DC/DC converter that regulates the SC operation have been also proposed [25], [26].

In contrast to all the referenced works, this paper proposes a strategy in which IE is achieved exclusively from the stored energy in an SC directly connected to the DC link, avoiding the use of an additional DC/DC converter. By not adding this converter, the solution becomes cheaper, more compact and more reliable. Furthermore, the proposed strategy offers important advantages over state-of-the-art and commercial strategies: the WT captures the maximum available wind power during the frequency event, it provides higher energy

efficiency, it can emulate inertia regardless of the wind speed conditions, it avoids the SFD, the WT immediately responds to a frequency event due to the SC fast dynamics, among others.

V. Proposed Inertia Emulation Strategy for DFIG and PMSG Wind Turbines

A. Description of the strategy

The IE strategy proposed in this paper includes an SC directly connected to the DC link of the back-to-back power converter. The energy stored in this SC is the single energy source for the IR emulation, avoiding the use of stored kinetic energy or blade pitching. The SC operation is controlled by regulating the DC link voltage setpoint. This strategy can be implemented in both PMSG and DFIG WTs.

Fig. 3(a) shows the control scheme for the proposed technique. This IE controller reacts to a frequency drop by setting the DC link voltage setpoint (V^*_{DC}) below the rated DC link voltage (V_{DCnom}). In both DFIG and PMSG, the grid-side converter (GSC) incorporates a control loop that ensures that the DC link voltage (V_{DC}) follows its setpoint, as shown in Fig. 3 (b). Then, a fraction of the SC stored energy is released and injected into the grid, emulating the IR. The magnitude of the additional output power is controlled by modifying k_{DC}. This control structure incorporates a low-pass filter to reject measurement noise; a high-pass filter to reject steady-state frequency errors; and a dead band to reject small perturbations in frequency during the normal operation of the system.

With the proposed IE strategy T_{em} remains constant during grid frequency excursions since T^*_{em} is not used as a control variable. This makes it possible to eliminate a restriction that conventional IE strategies, based on pitch control and kinetic energy variations, present while rotating at low speeds. With these strategies, an underfrequency event results in an increased T_{em}, which leads to a drop in speed. Turbine deceleration reduces aerodynamic lift, aggravating the speed drop. This positive feedback pushes the blades towards aerodynamic stall, which needs to be avoided. IE is limited for low Ω to provide a margin above the stall [17].

As T_{em} remains constant, there is no torque imbalance during a frequency deviation, i.e., there is no speed variation. This feature makes it possible to remain operating at the MPP, which leads to an augmented annual energy production (AEP) and avoids the SFD. Furthermore, it favors the omission of another limitation shown by conventional IE strategies. To avoid abrupt Ω changes that cause mechanical stress on the drive train and reduce the WT lifetime, the rate of change of output power is limited, which should not exceed 0.45 p.u./s [8].

The ability to keep operating at the MPP also aids in rapid grid frequency return to nominal value. During the speed recovery process associated with conventional IE techniques, WT output power is lower than the power it was injecting into the grid before the underfrequency event, as it is not operating at the MPP and a fraction of the captured mechanical power is being used to accelerate the machine. The primary regulation service contributes with additional power support to compensate this generation loss. It is crucial that the speed recovery process takes place just after the event, as WTs need to return to the MPP as soon as possible in order to minimize the aforementioned generation loss. The higher demand on the primary regulation service delays the frequency recovery to the nominal value [22]. With the proposed strategy, the recovery process (associated with the SC charging phase) does not need to occur just after the event, as the turbines remain operating at the MPP. Recovery could start once the frequency has reached its nominal value. This means that, after the period of increased output power, the WT output power could be equal to the power it was injecting into the grid before the event, without overloading the primary regulation service and avoiding a delay in frequency recovery.

The use of the energy stored in the SC offers maximum capacity to emulate inertia regardless of the wind speed conditions, even when the WT is stopped. This is not feasible when implementing conventional IE approaches. Limitations appear if an underfrequency event when wind speed is lower than its cut-in speed (WT is stopped), equal or slightly higher than its cut-in speed (WT is rotating at Ω_{min} or close to it) or higher than its cut-out speed (WT is stopped). If the turbine is stopped, then there is no kinetic energy stored in the rotating masses. Therefore, there is no IR available. The turbine speed must remain within its operating range Ω_{min}-Ω_{max} (0.5-1.2 p.u. for PMSG and 0.7-1.2 p.u. for DFIG [8]). Therefore, if the WT is rotating at Ω_{min} or close to it, its deceleration is restricted, so the available IR is either zero or very limited.

With the proposed IE strategy, the turbine output power changes almost immediately hen a frequency event is detected, due to the SC's fast charge/discharge dynamics. However, the slow nature of mechanical pitch angle controller system delays the response of state-of-the-art strategies [26]. In this case, the proposed strategy better mimics the sudden IR of a grid-tied synchronous generator, favoring the replacement of these generators with WTs.

Placing the IE energy source in the DC link of the back-to-back converter increases the energy efficiency of the solution. To achieve the same additional output power, the amount of kinetic energy that the WT rotating masses have to release is higher than the energy that the SC has to discharge. The reason is that the mechanical losses in the drive train added to the electrical losses in the generator and back-to-back converter (in both RSC and GSC) are greater than the SC discharge losses added to the GSC electrical losses.

B. Sizing of the supercapacitor and tuning of k_{DC}

The additional power required to provide virtual inertia during a frequency drop is proposed to be extracted from a SC connected to the DC link. The sizing of this SC needs to be done taking into account a dimensioning frequency event extracted from the grid code. The parameters required for this sizing are the maximum RoCoF that the wind turbine needs to face ($RoCoF_{max}$), the power surplus that the turbine needs

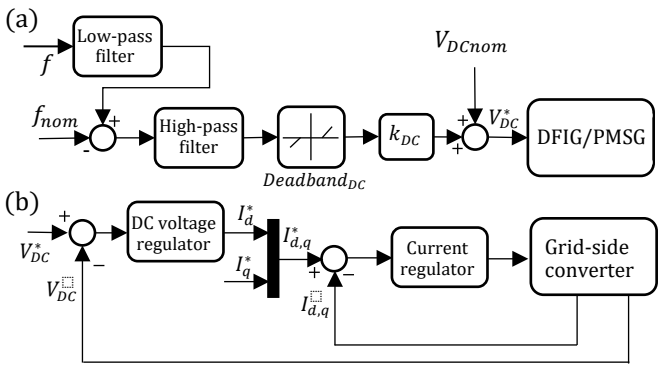

Fig. 3. Generalised control scheme for the proposed IE technique: (a) proposed control loop for the supercapacitor voltage and (b) typical vector control loop for the GSC.

to provide with this $RoCoF_{max}$ (ΔP_{max}), and the maximum time required for the inertia emulation (t_{P+}).

The sizing of the SC is done by means of an energy analysis, taking into account that ΔP_{max} needs to be provided only at $RoCoF_{max}$, and the remaining time of t_{P+} the power increases and decreases, almost linearly, to 0. Therefore, the required energy can be estimated as follows:

$$E_{IE} = \frac{\Delta P_{max} \cdot t_{P+}}{2} \tag{5}$$

On the other hand, the energy stored in a SC depends on the square of its voltage. If the SC voltage before the frequency event is $V_{DC,N}$, and the minimum DC bus voltage is $V_{DC,min}$, the energy extracted from the SC during the dimensioning frequency event is:

$$E_{SC} = \frac{1}{2} C \left(V_{DC,N}^2 - V_{DC,min}^2 \right) \tag{6}$$

Therefore, the capacitance required to perform the proposed IE strategy is:

$$C = \frac{\Delta P_{max} \cdot t_{P+}}{\left(V_{DC,N}^2 - V_{DC,min}^2 \right)} \tag{7}$$

Once the capacitance is known, k_{DC} needs to be tuned for the required power to be delivered at the desired RoCoF. k_{DC} is the proportional gain that relates f with V_{DC} or, alternatively, $RoCoF = \frac{df}{dt}$ with $\frac{dV_{DC}}{dt}$. $\frac{dV_{DC}}{dt}$ can be related with the DC-link power (P_{DC}) as follows:

$$P_{DC} = \frac{dE_{SC}}{dt} = \frac{d}{dt}\left(\frac{1}{2} C\, V_{DC}^2\right) = C\, V_{DC} \frac{dV_{DC}}{dt}, \tag{8}$$

being E_{SC} the energy stored in the DC bus and V_{DC} the bus voltage. Particularizing Eq. (8) to the dimensioning frequency event (P_{DC}= ΔP_{max}), and considering $RoCoF = RoCoF_{max}$, k_{DC} can be calculated as follows:

$$k_{DC} = \frac{\frac{dV_{DC}}{dt}}{\frac{df}{dt}} = \frac{\Delta P_{max}}{RoCoF_{max}\, C\, V_{DC,nom}} \tag{9}$$

VI. Performance Analysis and Discussion

This section aims to compare the IR of a DFIG (VI. B) and a PMSG (VI. C). Three cases are compared for each of the wind turbines: their natural response with no IE strategy, a state-of-the-art IE technique and the IE strategy proposed in this paper.

A. Description of the scenario

The frequency event selected for the comparison is shown in Fig. 4(a) and Fig. 5(a), which illustrates the evolution of the Continental European Power System frequency in the event of a 3 GW generation loss, as proposed by ENTSO-E [27]. This is the dimensioning incident for the primary regulation service control and is also used in this study to size the proposed IE strategy. At the time of this event, 107 GW out of the 405 GW total load are supplied by wind power, representing a high 26.4% of wind penetration. The required parameters for this sizing frequency event are $RoCoF_{max}$ = –0.075 Hz/s, ΔP_{max} = 0.05 p.u., and t_{P+} = 20 s.

For the DFIG response analysis, a 1.6-MW DFIG model available in the Mathworks documentation with an inertia H = 5 s is used. The machine has a nominal speed Ω_N = 1000 rpm, nominal voltage $V_{N,L\text{-}L}$ = 690 V and nominal torque T_N = 15.3 kNm. The detailed parameters of this model can be accessed in the Mathworks Simscape Electrical documentation webpage [28]. The DFIG includes a rotational speed closed loop MPPT, like the one shown in Fig. 1(b). The analysis is carried out with a constant wind speed of 12 m/s. Under these wind speed conditions, before the frequency event, the DFIG rotates at a speed of 1.2 p.u. and the output power is 0.79 p.u. For the PMSG performance analysis, a 1.5-MW direct-driven PMSG model is used, with the same inertia H = 5 s, a nominal speed Ω_N = 62.5 rpm, nominal voltage $V_{N,L\text{-}L}$ = 575 V and nominal torque T_N = 230 kNm. The model is also available on the Mathworks documentation webpage [29]. It includes an open-loop MPPT, like the one shown in Fig. 1(a). The analysis is made with a constant wind speed of 11 m/s. Before the frequency event, the PMSG rotates at a speed of 1 p.u. and outputs a power of 0.735 p.u.

In order to study the response of both WTs with conventional IE, a representative IE strategy used in commercial solutions and based on an FFR technique is implemented [6], [17]. The DC link capacitance for both wind turbines is 10 mF. Then, based on Fig. 2(a) and 2(b), $k_{df/dt}$ is set to zero. $k_{\Delta f}$ is tuned to respond to this frequency event with a maximum additional output power of 0.05 p.u. The DFIG, $Deadband_{\Delta f}$ is set to ±0.0025 p.u. (as proposed in [17]) to react only to large frequency excursions, for which IR is relevant to ensure grid stability. In the PMSG, $Deadband_{\Delta f}$ is set to zero. For the implementation of the proposed strategy,

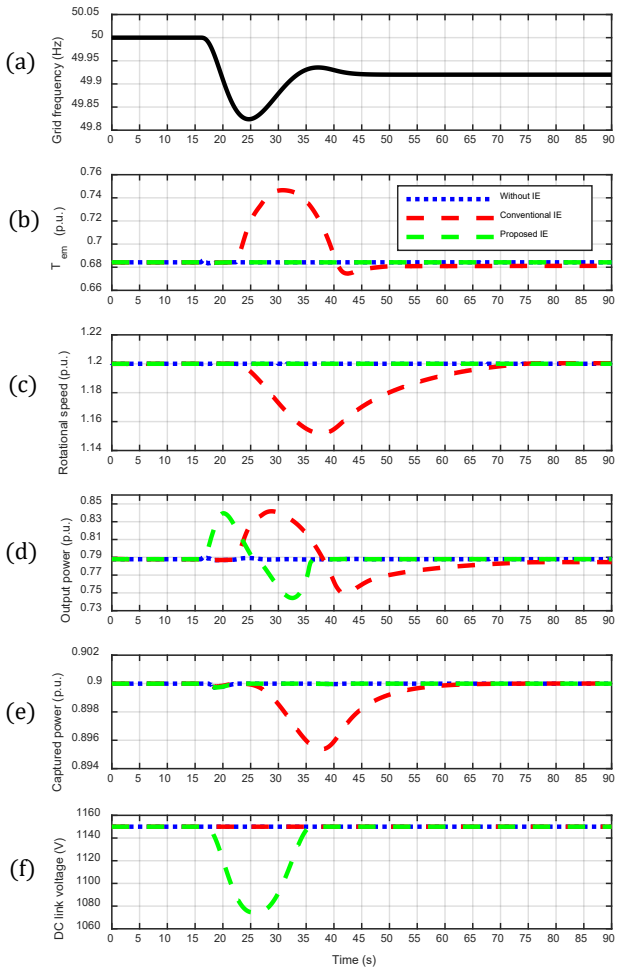

Fig. 4. Results for the DFIG inertial response comparison: (a) grid frequency (Hz); (b) T_{em} (p.u.); (c) WT rotational speed (p.u.); (d) WT output power (p.u.); (e) Captured power by the WT rotor (p.u.); (f) Back-to-back converter DC link voltage (V).

shown in Fig. 3, the capacitance of the SC needs to be calculated. Considering the values of ΔP_{max} = 0.05 p.u. = 75 kW, $t_{P+} = 20$ s, $V_{DC,N} = 1150$ V and $V_{DC,min} = 1000$ V, the SC capacitance obtained from Eq. (7) is 4.65 F. Subsequently, k_{DC} is computed based on Eq. (9), considering the $RoCoF_{max} = -0.075$ Hz/s, the obtained value is $k_{DC} = -187$ V/Hz. Moreover, $Deadband_{DC}$ is set to zero in order to react to all events.

B. DFIG performance analysis

With the DFIG in its standard configuration (without IE), Fig. 4(b) shows that T_{em} does not change when the grid frequency is reduced. The controller $G_{\Omega}(s)$ reacts to this deceleration, and the RSC keeps a constant T_{em}. Due to the immediate response of $G_{\Omega}(s)$, Ω variation associated with this T_{em} transient is minimal. This minor Ω variation is not even perceived in Fig. 4(c), but its effect is seen in Fig. 4(e), where the WT is not able to capture the maximum available wind power as it has been forced to leave the MPP. Since the WT immediately re-operates at the MPP, the captured energy loss is minimal. As $G_{\Omega}(s)$ does not allow a significant release of the kinetic energy stored in the rotating masses of the WT, the increase in output power is insignificant, as shown in Fig. 4(d). Fig. 4(f) illustrates that the DC link voltage remains constant at its nominal value (1150 V).

With the conventional IE strategy, once the frequency leaves the $Deadband_{\Delta f}$ range, the IE controller reacts by adding ΔT^*_{em}. T_{em} follows its setpoint, being greater than its original value for 18 s, as shown in Fig. 4(b). During this time, the WT is decelerated due to the torque imbalance (Fig. 4(c)). The released kinetic energy is injected into the grid, so the WT outputs an additional amount of power during those 18 s (Fig. 4(d)), reaching 0.84 p.u. After these 18 s, $G_{\Omega}(s)$ reacts to the Ω deviation and tries to recover its original speed (1.2 p.u.) by providing a T^*_{em} lower than its original value (Fig. 4(b)). The WT accelerates due to the torque imbalance (Fig. 4(c)). During the recovery, WT output power is lower than the power injected into the grid before the frequency event since a fraction of captured power is spent on accelerating the machine (Fig. 4(d)). Fig. 4(e) illustrates that, from the moment when the IE controller reacts to the frequency event until the end of the recovery, the machine operates outside the MPP, which means that the captured power is not optimal. Fig. 4(f) shows how the DC link voltage remains constant at 1150V.

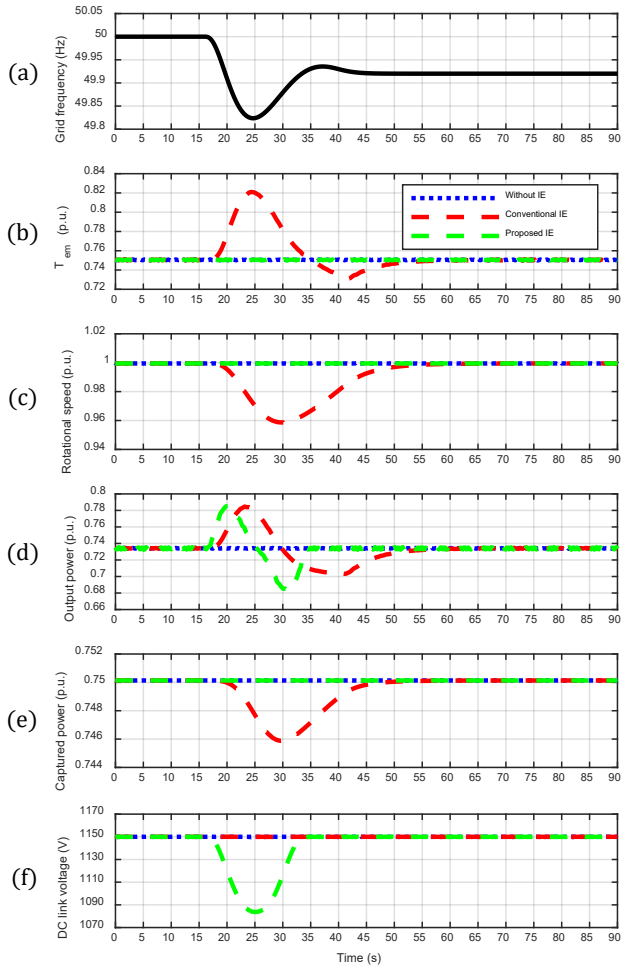

Fig. 5. Results for the PMSG inertial response comparison: (a) grid frequency (Hz); (b) T_{em} (p.u.); (c) WT rotational speed (p.u.); (d) WT output power (p.u.); (e) Captured power by the WT rotor (p.u.); (f) Back-to-back converter DC link voltage (V).

With the proposed IE strategy, Fig. 4(b) illustrates that T_{em} responds in the same way as when there is no IE strategy implemented, since T^*_{em} is not used as a control variable to achieve the IR. Therefore, the rotating speed (Fig. 4(c)) and the captured power (Fig. 4(e)) also evolve identically. As $Deadband_{DC}$ has not been included for this simulation, the IE controller reduces V^*_{DC} from the start of the frequency event. The GSC forces V_{DC} to follow V^*_{DC}, as shown in Fig. 4(f). V_{DC} decreases for 9 seconds until the maximum frequency deviation from 50 Hz is reached (Nadir frequency). During this time interval, the power released from the SC is injected into the grid, so the WT outputs an additional amount of power, as shown in Fig. 4(d). As in the previous case, the maximum turbine output power is 0.84 p.u., which corresponds to an extra amount of 5% of rated power. After Nadir frequency, Fig. 4(d) shows that output power is lower than the injected power into the grid before the frequency event since a fraction of the captured power is spent on charging the SC (recovery period). Recovery lasts until V_{DC} reaches 1150V, 9 s in this case (Fig. 4(f)). Compared to conventional IE, a shorter recovery period is achieved.

C. PMSG performance analysis

With the PMSG in its standard configuration (without IE), Fig. 5(b) shows that T_{em} is not sensitive to frequency variations. As there is no torque imbalance, Ω remains unvarying, as shown in Fig. 5(c). Since the speed of the WT is not modified, it keeps operating at the MPP, capturing the maximum available wind power (Fig. 5(e)). Fig. 5(d) illustrates that the WT output power stays constant, as no kinetic energy is released from the rotating masses of the WT. Fig 5(f) shows that DC link voltage remains at its nominal value (1150 V).

With the conventional IE strategy, the controller reacts to a frequency drop by adding ΔP^*_{out}. This leads to a T_{em} greater than its original value for 18 s, as shown in Fig. 5(b). During this time, the WT is decelerated due to the torque imbalance (Fig. 5(c)). At the same time, the released kinetic energy is injected into the grid, so the WT power increases (Fig. 5(d)). Afterwards, the speed recovery period starts and lasts for 26 s. During the recovery, T_{em} is lower than its original value (Fig. 5(b)), so the WT accelerates due to the torque imbalance (Fig. 5(c)). The WT output power is lower than the injected power into the grid before the frequency event since a fraction of the captured power is used to accelerate the turbine (Fig. 5(d)). The WT operates outside the MPP during this time, with a captured power lower than optimal (Fig. 5(e)). Fig. 5(f) illustrates that the DC link voltage does not vary.

With the proposed IE strategy, T^*_{em} is not used as the control variable to achieve the IR. Thus, T_{em} remains constant, as shown in Fig. 5(b). As there is no torque imbalance, the rotational speed does not change (Fig. 5(c)). The WT operates at the MPP during the entire frequency event, capturing the maximum available wind power (Fig. 5(e)). When the frequency starts to decrease, the IE controller reacts by reducing V^*_{DC} for 9 s, until Nadir frequency is reached. V_{DC} follows V^*_{DC}, as shown in Fig. 5(f). During this time interval, the WT outputs an additional amount of power (Fig. 5(d)), since the released energy from the SC is injected into the grid. After these 9 s, the recovery period starts and has a time duration of 9 s. During the recovery, a fraction of captured power is spent on charging the SC. Then, output power is lower than the injected power into the grid before the frequency event (Fig. 5(d)). Recovery ends when V_{DC} reaches 1150 V again (Fig. 5(f)). As in the DFIG case, a shorter recovery period is achieved compared to conventional IE.

VII. Conclusions

Conventional power plants are mostly based on grid-tied synchronous generators. The IR of these generators, which consists of an inherent change in their rotational speed and output power when facing a grid frequency variation, contributes to grid stability. Various TSOs require WPPs to emulate inertia in order to keep a suitable frequency response. The most common technique implemented in state-of-the-art WTs for IE relies on pitch control and kinetic energy variations. An IE strategy valid for both PMSG and DFIG is proposed in this paper. This IE achieves a change in the output power by varying the charge of an SC connected to the back-to-back converter DC link.

The performance of the proposed IE strategy has been simulated for DFIG and PMSG WT topologies, thereby proving its advantages over state-of-the-art strategies. The most relevant advantage is that it does not require a modification of the WT speed and torque. Therefore, the maximum power point is not left, and the WT captures the maximum available wind power during the frequency event, leading to a higher energy efficiency and to the prevention of a potential secondary frequency drop, which can be even more harmful than the first frequency event. Moreover, this constant torque alleviates the mechanical stress of the drive train, thereby enlarging the turbine lifetime. Another advantage of the proposed IE strategy is that it can be used at any wind conditions, even for a low wind speed that prevents the application of state-of-the-art strategies to avoid aerodynamic stall.

While the proposed IE strategy outperforms conventional IE approaches, it does require the inclusion of an additional component (the SC), which increases the initial investment of the solution. The SC market is experiencing a remarkable expansion, accompanied by intensive research and development aimed at reducing costs. The decreasing prices of SCs makes the proposed IE strategy increasingly competitive.

To sum up, through the inclusion of an SC, the IE strategy proposed in this paper allows WTs to provide virtual inertia, facing frequency deviations with higher accuracy than previous strategies, thereby favoring the replacement of traditional generators by WTs.

References

[1] J. Machowski, J. W. Bialek, and J. R. Bumby, "Power System Dynamics. Stability and Control," 3rd ed. Hoboken (NJ), USA: John Willey & Sons, 2012.

[2] A. Mullane and M. O'Malley, "The inertial response of induction-machine-based wind turbines," *IEEE Trans. Power Syst.*, vol. 20, no. 3, pp. 1496–1503, 2005, doi: 10.1109/TPWRS.2005.852081.

[3] A. Mullane, G. Bryans, and M. O'Malley, "Kinetic energy and frequency response comparison for renewable generation systems," in *2005 Int. Conf. on Future Power Syst.*, 2005, p. 6, doi: 10.1109/FPS.2005.204252.

[4] N. Goñi, J. Sacristán, A. Berrueta, J. L. Rodríguez, A. Ursúa, and P. Sanchis, "New design alternatives for a hybrid photovoltaic and doubly-fed induction wind plant to augment grid penetration of renewable energy," in *IEE EEEIC and CPS Europe*, Bari, Italy, 2021, pp. 1-6, doi: 10.1109/EEEIC/ICPSEUROPE51590.2021.9584546.

[5] F. Gonzalez-Longatt, "Impact of synthetic inertia from wind power on the protection/control schemes of future power systems: Simulation study," *IET Conference Publications*, vol. 2012, no. 593 CP, 2012, doi: 10.1049/cp.2012.0030.

[6] M. Fischer, S. Engelken, N. Mihov, and A. Mendonca, "Operational experiences with inertial response provided by type 4 wind turbines," *IET Renewable Power Generation*, vol. 10, no. 1, pp. 17–24, 2016, doi: 10.1049/iet-rpg.2015.0137.

[7] ENTSO-E, "Commission Regulation (EU) 2016/631 of 14 April 2016 establishing a network code on requirements for grid connection of generators," *Official Journal of the European Union*, no. 14 April 2016, pp. 1–68, 2016.

[8] Z. Wu *et al.*, "State-of-the-art review on frequency response of wind power plants in power systems," *J. of Modern Power Systems and Clean Energy*, vol. 6, no. 1, pp. 1–16, 2018, doi: 10.1007/s40565-017-0315-y.

[9] J. Sacristán *et al.*, "Inertial Response and Inertia Emulation in DFIG and PMSG Wind Turbines: Emulating Inertia from a Supercapacitor-based Energy Storage System," n *IEE EEEIC and CPS Europe*, Bari, Italy, 2021, pp. 1-6, doi: 10.1109/EEEIC/ICPSEurope51590.2021.9584753.

[10] A. Berrueta, I. San Martín, P. Sanchis, and A. Ursúa, "Lithium-ion batteries as distributed energy storage systems for microgrids," in *Distributed Energy Resources in Microgrids: Integration, Challenges and Optimization*, Elsevier, 2019, pp. 143–183. doi: 10.1016/B978-0-12-817774-7.00006-5.

[11] H. Beltran, S. Harrison, A. Egea-Álvarez, and L. Xu, "Techno-economic assessment of energy storage technologies for inertia response and frequency support from wind farms," *Energies*, vol. 13, no. 13, Jul. 2020, doi: 10.3390/en13133421.

[12] A. Soto, A. Berrueta, M. Mateos, P. Sanchis, and A. Ursúa, "Impact of micro-cycles on the lifetime of lithium-ion batteries: An experimental study," *J Energy Storage*, vol. 55, no. 105343, Nov. 2022, doi: 10.1016/j.est.2022.105343.

[13] A. Soto, A. Berrueta, I. Oficialdegui, P. Sanchis, and A. Ursúa, "Noninvasive Aging Analysis of Lithium-Ion Batteries in Extreme Cold Temperatures," *IEEE Trans Ind Appl*, vol. 58, no. 2, pp. 2400–2410, 2022, doi: 10.1109/TIA.2021.3136808.

[14] A. Berrueta, A. Ursúa, I. S. Martin, A. Eftekhari, and P. Sanchis, "Supercapacitors: Electrical Characteristics, Modeling, Applications, and Future Trends," *IEEE Access*, vol. 7, pp. 50869–50896, 2019, doi: 10.1109/ACCESS.2019.2908558.

[15] G. Abad, J. Lopez, M. A. Rodriguez, L. Marroyo, and G. Iwanski, "Doubly Fed Induction Machine: Modeling and Control for Wind Energy Generation" Wiley-IEEE Press, 2011, ISBN: 9781118104965.

[16] A. Sachan, A. K. Gupta, and P. Samuel, "A review of MPPT algorithms employed in wind energy conversion systems," J. *Green Eng.*, vol. 6, no. 4, pp. 385–402, 2017, doi: 10.13052/jge1904-4720.643.

[17] K. Clack, N. W. Miller and J. J. Sanchez-Gasca, "Modeling of GE Wind Turbine-Generators for Grid Studies," General Electric International, Inc., 2010.

[18] N. W. Miller, K. Clark, and M. Shao, "Frequency responsive wind plant controls: Impacts on grid performance," *IEEE Power and Energy Soc General Meeting*, pp. 1–8, 2011, doi: 10.1109/PES.2011.6039137.

[19] X. Yan and X. Sun, "Inertia and droop frequency control strategy of doubly-fed induction generator based on rotor kinetic energy and supercapacitor," *Energies*, vol. 13, no. 14, 2020, doi: 10.3390/en13143697.

[20] J. Hossain and A. Mahmud, *Large Scale Renewable Power Generation*, Springer, 2014. ISBN: 978-9814585293.

[21] J. Van De Vyver, J. D. M. De Kooning, B. Meersman, L. Vandevelde, and T. L. Vandoorn, "Droop Control as an Alternative Inertial Response Strategy for the Synthetic Inertia on Wind Turbines," *IEEE Trans. Power Syst.*, vol. 31, no. 2, pp. 1129–1138, 2016, doi: 10.1109/TPWRS.2015.2417758.

[22] S. G. Kim and M. Bollen, "On some aspects of power system stability and grid code requirements relevant for large scale grid power integration," in Elforsk Rapport 13:04, Stockholm, 2013.

[23] J. Licari, J. Ekanayake, and I. Moore, “Inertia response from full-power converter-based permanent magnet wind generators,” *J. Modern Power Syst. and Clean Energy*, vol. 1, no. 1, pp. 26–33, 2013, doi: 10.1007/s40565-013-0002-6.

[24] L. Xiong, Y. Li, Y. Zhu, P. Yang, and Z. Xu, “Coordinated control schemes of super-capacitor and kinetic energy of DFIG for system frequency support,” *Energies*, vol. 11, no. 1, 2018, doi: 10.3390/en11010103.

[25] X. Yan and X. Sun, “Inertia and droop frequency control strategy of doubly-fed induction generator based on rotor kinetic energy and supercapacitor,” *Energies*, vol. 13, no. 14, 2020, doi: 10.3390/en13143697.

[26] M. F. M. Arani and E. F. El-Saadany, “Implementing virtual inertia in DFIG-based wind power generation,” *IEEE Trans. on Power Syst*, vol. 28, no. 2, pp. 1373–1384, 2013, doi: 10.1109/TPWRS.2012.2207972.

[27] ENTSO-E, “Inertia and Rate of Change of Frequency (RoCoF),” *Executive summary*, 2020.

[28] R. Gagnon, “Wind Farm - DFIG Detailed Model Matlab Simulink,” MATLAB Central File Exchange. [Online]. Available: https://es.mathworks.com/help/sps/ug/wind-farm-dfig-detailed-model.html.

[29] R. Jiayang, “Detailed Modelling of a 1.5 MW Wind Turbine based on Direct-driven PMSG,” MATLAB Central File Exchange. [Online]. Available: https://www.mathworks.com/matlabcentral/fileexchange/41833-detailed-modelling-of-a-1-5mw-wind-turbine-based-on-direct-driven-pmsg.